

Magnetic phase diagrams of $\text{Ce}_2\text{Fe}_{17-x}\text{Mn}_x\text{-H}$ system: A magnetization study

W. Iwasieczko^{a,*}, A.G. Kuchin^{b,c}, L. Folcik^a, H. Drulis^a

^a Polish Academy of Science, Trzebiatowski Institute of Low Temperature and Structure Research,
59-950 Wrocław 2, P.O. Box 1410, Poland

^b Institute for Metal Physics, S. Kovalevskay 18, 620219 Ekaterinburg, Russia

^c International Laboratory of High Magnetic Fields and Low Temperature, Gajowicka 95,
53-421 Wrocław, Poland

Received 13 July 2004; received in revised form 4 January 2005; accepted 10 January 2005
Available online 20 July 2005

Abstract

The field-induced magnetic phase transitions of the helical phase of $\text{Ce}_2\text{Fe}_{17-x}\text{Mn}_x$ alloys ($x = 1.3$ and 1.7) and their hydrides of $\text{Ce}_2\text{Fe}_{17-x}\text{Mn}_x\text{H}_y$ ($y = 1$) were investigated by isofield magnetization curves in external magnetic fields up to $H = 10$ kOe. The temperature dependence of the critical fields, H_C inducing phase transition between ferromagnetic (F) and helical antiferromagnetic (HAFM) state are determined. On the basis of the experimental results, the H - T phase diagrams are established. The multiple magnetic phase transitions observed in the low magnetic field are discussed in terms of competing exchange contributions within the iron magnetic sublattices. Hydrogenation leads to a considerable enhancement of ferromagnetic-like exchange interactions, which causes the increase of the Curie temperature and drastically reduces the critical field H_C of a metamagnetic transition.

© 2005 Elsevier B.V. All rights reserved.

Keywords: Metamagnetism; Rare earth-iron hydrides; Magnetic phase diagrams

1. Introduction

Among the binary R_2Fe_{17} compounds the $\text{Ce}_2\text{Fe}_{17}$ and its solid solutions with other 3d metals exhibit unique magnetic properties [1]. A general characteristic of binary $\text{Ce}_2\text{Fe}_{17}$ compound is that the cerium atoms carry no magnetic moment [2] hence the Fe sublattice fully determines the magnetic properties. Previous neutron diffraction studies [1] have shown that $\text{Ce}_2\text{Fe}_{17}$ compound undergoes successive magnetic phase transitions, accompanied by changes of the ordering mode which is from paramagnetic state to helicoidal antiferromagnetic and finally to the ferromagnetic spin structure at low temperatures. The thermal variation of the magnetization under a field of 100 Oe for $\text{Ce}_2\text{Fe}_{17}$ is peculiar [3]. A magnetization peak characteristic of a Néel temperature is observed at $T_N = 206$ K. Another anomaly

at $T_T = 94$ K where magnetization strongly increases corresponds to the spontaneous magnetization characteristic for ferromagnetic ordering. In the antiferromagnetic helical phase between T_N and T_T the magnetic moments form ferromagnetic layers with a resulting magnetization parallel to the basal plane. The direction of the magnetic moments of the layers rotates from layer to layer according to a temperature dependent angle of rotation. Such an arrangement of magnetic moments is due to a compromise between positive and negative Fe–Fe exchange interactions. It is well known that in magnetic iron compounds, the Fe–Fe distances and the number of nearest neighbour Fe atoms play essential roles. It has been established that in $\text{Ce}_2\text{Fe}_{17}$ the magnetic structure is determined by the shortest Fe–Fe interactions [1].

The intermetallic $\text{R}_2\text{Fe}_{17-x}\text{Mn}_x$ solid solution with the manganese have attracted large attention because of the very interesting magnetic behaviour. For example, in $\text{Gd}_2\text{Fe}_{17-x}\text{Mn}_x$ compounds, the Mn moments are coupled

* Corresponding author. Tel.: +48 71 34 350 21; fax: +48 71 441 029.
E-mail address: iwasiecz@int.pan.wroc.pl (W. Iwasieczko).

antiparallel to Fe moments and carry up $3 \mu_B$ [4]. Substitution of Mn for Fe causes a monotonic decrease of the Curie temperature and the saturation magnetization in the $\text{Nd}_2\text{Fe}_{17-x}\text{Mn}_x$ compounds [5]. Neutron diffraction studies of $\text{Ce}_2\text{Fe}_{17-x}\text{Mn}_x$ solid solution show that Mn prefers the 6c site and avoid completely the 9d site, whereas the 18f and 18h sites are occupied almost randomly [6]. Mn, as a third component can essentially influence the magnetic state of $\text{Ce}_2\text{Fe}_{17-x}\text{Mn}_x$ solid solution due to the existence of three different exchange interactions: Fe–Mn, Mn–Mn and Fe–Fe. It has been found that the Néel temperature of the $\text{Ce}_2\text{Fe}_{17-x}\text{Mn}_x$ compounds decreases monotonously with the Mn content increasing in the range of $0 < x < 2$. Whereas the variation of the antiferro-ferromagnetic transition temperature, T_T , is non-monotonous. The low temperature ferromagnetic state of the parent compound gradually vanishes when x increases from $x = 0$ to 0.5. Finally, the compounds appear as antiferromagnets at all temperatures below T_N for x comprised between 0.5 and 1.0. Surprisingly, a re-entrance of ferromagnetic ordering takes place again when the Mn concentration reaches $x \cong 1.3$ [7,8]. Then, T_T is shifted to higher temperatures with the Mn content increasing [6].

To enlighten more the complex magnetic behavior of the $\text{Ce}_2\text{Fe}_{17-x}\text{Mn}_x$ system we performed magnetization measurements versus temperature in different applied magnetic fields. On the basis of these data a magnetic phase diagrams were constructed. Besides, we also studied the influence of hydrogenation on structural and magnetic properties of selected $\text{Ce}_2\text{Fe}_{17-x}\text{Mn}_x$ compounds, which may lead to a better understanding of magnetic states existing in this system.

2. Experimental details

$\text{Ce}_2\text{Fe}_{17-x}\text{Mn}_x$ ($x = 1.3$ and 1.7) compounds were prepared by induction melting Fe and Mn of 99.99% purity and Ce metals of 99.5% purity, with subsequent annealing of the ingots at 900°C for three days. X-ray powder diffraction was employed to determine the phase composition, the structure and the lattice parameters.

The hydrides $\text{Ce}_2\text{Fe}_{17-x}\text{Mn}_x\text{H}_y$ with hydrogen concentration $y = 1, 2$ and 3 were prepared using a vacuum glass apparatus through the direct absorption of hydrogen by the

compounds after a short thermal activation procedure at 500°C . At this temperature high purity hydrogen obtained by the thermal decomposition of titanium hydride was admitted at a given pressure to reach the expected stoichiometry. To achieve good homogenization, the product was slowly cooled down (about 20 K/h) to room temperature. The hydrogen concentration was determined by a volumetric method with an accuracy of ± 0.02 hydrogen atom per formula unit.

All the studied samples were controlled by X-ray diffraction using DRON diffractometer with $\text{Co K}\alpha$ radiation. The magnetization measurements were carried out using a SQUID magnetometer in the temperature range of $1.7\text{--}350\text{ K}$ and in magnetic fields up to 50 kOe . The magnetization curves were recorded on the bulk samples not free to rotate in the sample holder.

3. Results and discussion

3.1. Structural analysis

X-ray powder diffraction patterns analysis has indicated that all the investigated $\text{Ce}_2\text{Fe}_{17-x}\text{Mn}_x$ compounds and their hydrides crystallize in the $\text{Th}_2\text{Zn}_{17}$ -type structure (space group ($R\text{-}3m$)). Besides, it appears that the fraction of free iron ($\alpha\text{-Fe}$) as impurity was not larger than 1 wt.% in starting alloys, but it is comprised between 5 and 7 wt.% after hydrogenation. The lattice parameters are presented in Table 1. It is worth to stress that hydrogenation does not change the crystal-type symmetry even for the highest values of hydrogen content. However, hydrogenation leads to a highly anisotropic cell expansion that takes place mainly in the hexagonal base plane.

Neutron diffraction analysis [9] has revealed that in R_2Fe_{17} ($\text{Th}_2\text{Zn}_{17}$ -type structure) hydrogen is accommodated in octahedral ($2R\text{-}4\text{Fe}$) and tetrahedral ($2R\text{-}2\text{Fe}$) sites. The hydrogen atoms in octahedral sites were found more stable than in the tetrahedral one. Such scheme of occupation causes the a -cell parameter to linearly increases with y the hydrogen concentration whereas the c -cell parameter remains almost constant (or slightly decreases up to $y = 3$). It is worth to note that the a -cell parameter expansion observed in our experiment agrees well with a progressive filling of the octahedral sites.

Table 1
Structural data of $\text{Ce}_2\text{Fe}_{17-x}\text{Mn}_x\text{H}_y$ compounds

Compound	a (Å)	c (Å)	V (Å ³)	$\Delta a/a_0$ (%)	$\Delta c/c_0$ (%)	$\Delta V/V_0$ (%)
$\text{Ce}_2\text{Fe}_{15.7}\text{Mn}_{1.3}$	8.500	12.393	775.4			
$\text{Ce}_2\text{Fe}_{15.7}\text{Mn}_{1.3}\text{H}_1$	8.528	12.408	781.5	0.3	0.1	0.79
$\text{Ce}_2\text{Fe}_{15.7}\text{Mn}_{1.3}\text{H}_2$	8.555	12.401	787.0	0.6	0.06	1.50
$\text{Ce}_2\text{Fe}_{15.7}\text{Mn}_{1.3}\text{H}_3$	8.581	12.416	791.8	0.9	0.18	2.11
$\text{Ce}_2\text{Fe}_{15.3}\text{Mn}_{1.7}$	8.497	12.410	775.9			
$\text{Ce}_2\text{Fe}_{15.3}\text{Mn}_{1.7}\text{H}_1$	8.523	12.412	780.8	0.3	0.02	0.63
$\text{Ce}_2\text{Fe}_{15.3}\text{Mn}_{1.7}\text{H}_2$	8.562	12.416	788.2	0.8	0.05	1.59
$\text{Ce}_2\text{Fe}_{15.3}\text{Mn}_{1.7}\text{H}_3$	8.592	12.439	795.2	1.1	0.23	2.48

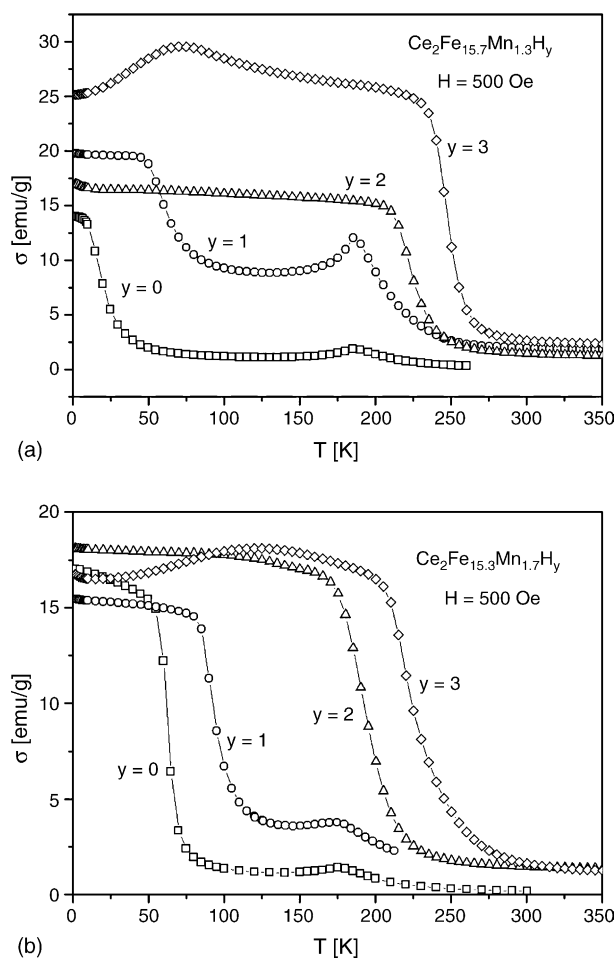


Fig. 1. (a) Magnetisation as a function of temperature for $\text{Ce}_2\text{Fe}_{15.7}\text{Mn}_{1.3}\text{H}_y$, and (b) for $\text{Ce}_2\text{Fe}_{15.3}\text{Mn}_{1.7}\text{H}_y$. The anomaly on the magnetization curves for the hydride with $y = 3$ will be discussed in a forthcoming paper.

3.2. Magnetic studies

Fig. 1 presents the magnetization dependence versus temperature of $\text{Ce}_2\text{Fe}_{15.7}\text{Mn}_{1.3}\text{H}_y$ and $\text{Ce}_2\text{Fe}_{15.3}\text{Mn}_{1.7}\text{H}_y$ hydrides ($y = 1, 2$ and 3) together with those of their parent compounds, in magnetic field of 500 Oe. These traces clearly demonstrate that hydrogenation changes the temperature of the ferro–antiferromagnetic phase transition, T_t , which rises with y increasing. Here, the T_t symbol was specially introduced to distinguish the helix–ferromagnetic transition from the para–ferromagnetic transition labelled by T_C . The Néel temperature is not so sensitive to hydrogen insertion as long as y is lower than 2. As is seen in Fig. 1 the antiferromagnetic–paramagnetic transition of the parent materials is no longer observed for the hydrides with $y > 2$. In the whole range of temperature and for all the applied fields, the $\text{Ce}_2\text{Fe}_{17}\text{Mn}_x\text{H}_y$ hydrides with $y > 2$ are ferromagnetic. The T_t and T_C determined as inflection points on the magnetization curves [10], and T_N defined as a maximum on the magnetization curves, are given in Table 2, versus y .

Table 2
Magnetic data of $\text{Ce}_2\text{Fe}_{17-x}\text{Mn}_x\text{H}_y$ compounds

Compound	T_N , (K)	T_t , (K)	T_C , (K)	$H_{C\max}$ (kOe)
$\text{Ce}_2\text{Fe}_{15.7}\text{Mn}_{1.3}$	187 ± 1	20 ± 2		7.5 ± 0.5
$\text{Ce}_2\text{Fe}_{15.7}\text{Mn}_{1.3}\text{H}_1$	187 ± 1	63 ± 2		4.5 ± 0.5
$\text{Ce}_2\text{Fe}_{15.7}\text{Mn}_{1.3}\text{H}_2$			225 ± 2	
$\text{Ce}_2\text{Fe}_{15.7}\text{Mn}_{1.3}\text{H}_3$			248 ± 2	
$\text{Ce}_2\text{Fe}_{15.3}\text{Mn}_{1.7}$	177 ± 1	62 ± 2		8.0 ± 0.5
$\text{Ce}_2\text{Fe}_{15.3}\text{Mn}_{1.7}\text{H}_1$	177 ± 1	94 ± 2		3.0 ± 0.5
$\text{Ce}_2\text{Fe}_{15.3}\text{Mn}_{1.7}\text{H}_2$			193 ± 2	
$\text{Ce}_2\text{Fe}_{15.3}\text{Mn}_{1.7}\text{H}_3$			228 ± 2	

It has been shown [1] that positive exchange interactions (ferromagnetic-like) are intensified in R_2Fe_{17} if the interatomic Fe–Fe distances become larger. It was found that in $\text{Ce}_2\text{Fe}_{17}$ the ferromagnetic phase is favoured when $d_{\text{Fe-Fe}}$ is larger than a critical value of 0.25 nm whereas antiferromagnetic phase is stabilized when $d_{\text{Fe-Fe}}$ is smaller than 0.24 nm [1]. From precise diffraction experiments performed on a series of R_2Fe_{17} hydrides it was shown that the most important changes in the Fe–Fe distances

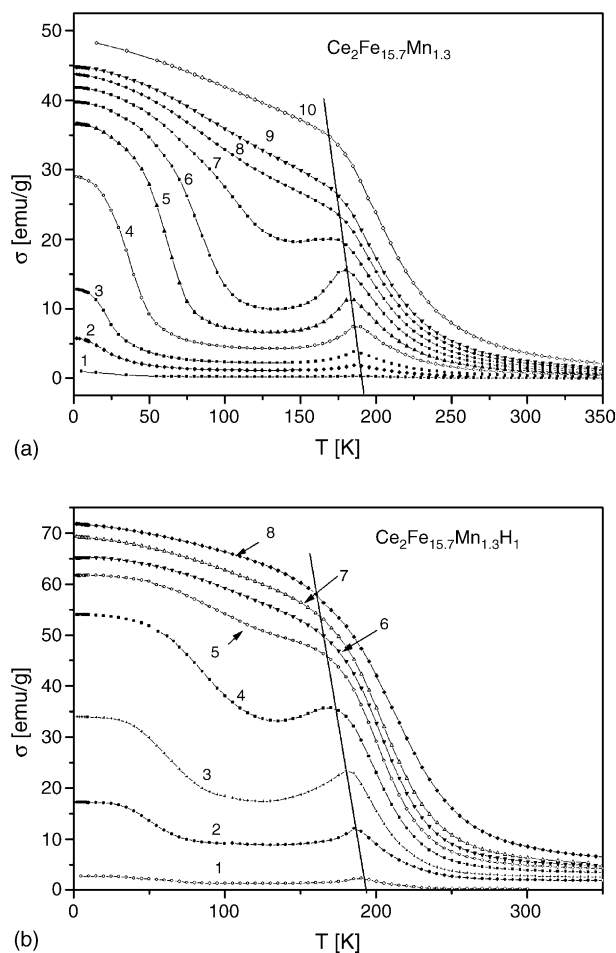


Fig. 2. (a) Temperature dependence of magnetization in various magnetic fields for $\text{Ce}_2\text{Fe}_{15.7}\text{Mn}_{1.3}$ (1–80 Oe; 2–500 Oe; 3–1 kOe; 4–2 kOe, 5–3 kOe, 6–4 kOe; 7–5 kOe; 8–6 kOe; 9–7 kOe; 10–10 kOe), and (b) for $\text{Ce}_2\text{Fe}_{15.7}\text{Mn}_{1.3}\text{H}_1$ (1–80 Oe; 2–500 Oe; 3–1 kOe; 4–2 kOe, 5–3 kOe, 6–4 kOe; 7–5 kOe; 8–6 kOe; 9–7 kOe; 10–10 kOe).

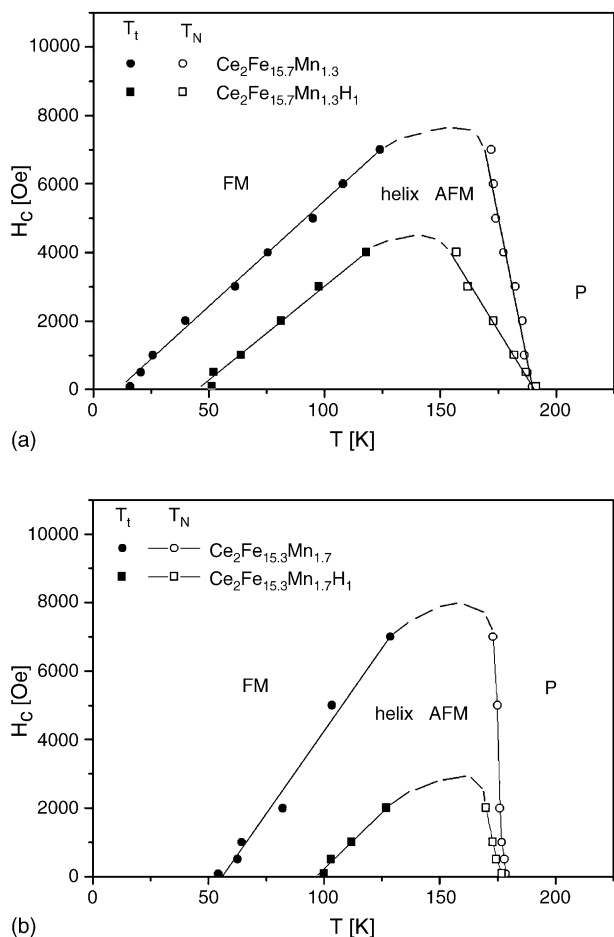


Fig. 3. The H - T magnetic phase diagrams for $\text{Ce}_2\text{Fe}_{15.7}\text{Mn}_{1.3}$ and $\text{Ce}_2\text{Fe}_{15.3}\text{Mn}_{1.7}$ compounds and their related hydrides with $y = 1$.

concerns the so-called dumbbell distances [11]. The positive exchange interactions appear to be much more intense when hydrogen atoms occupy the octahedral site i.e. when the Fe_1 - Fe_1 short distance (parallel to the c -axis), is markedly expanded. The increase of T_t and its final transformation to T_C in $\text{Ce}_2\text{Fe}_{17}\text{Mn}_x\text{H}_y$ hydrides can likely be correlated to the expansion of the Fe_1 - Fe_1 dumbbell distance.

The antiferromagnetic-ferromagnetic transition temperature, T_t , depends on the exchange interaction between the basal planes containing the Fe and Mn atom. It can be positive or negative, but its sign is determined by the atomic distances between these planes [12]. When this distance increases upon hydrogenation [13,14] the exchange interaction becomes positive and ferromagnetic couplings prevails in the hydride with $y \gg 2$.

The characteristic features of the magnetization curves for both the $\text{Ce}_2\text{Fe}_{17-x}\text{Mn}_x$ compounds and their $\text{Ce}_2\text{Fe}_{17}\text{Mn}_x\text{H}_y$ hydrides with $y = 1$ are specially interesting in temperature ranging between T_t and T_N . It is the unique range of temperature where the HAFM phase is stable. Additionally, magnetic phase transitions can be induced by means of magnetic field. To study the influence of

magnetic field on critical temperatures we have carried out magnetization measurements, σ versus T in various magnetic fields. For example in Fig. 2, the selected typical isofield magnetization curves are presented for $\text{Ce}_2\text{Fe}_{15.7}\text{Mn}_{1.3}$ and $\text{Ce}_2\text{Fe}_{15.7}\text{Mn}_{1.3}\text{H}_{1.0}$. From these typical traces the thermal dependence of H_c the critical field transitions between ferromagnetic, helical, and paramagnetic states were established. T_t can be determined only approximately, because the transition between the two regions takes place continuously. The corresponding H - T phase diagrams are presented in Fig. 3. For fields $H > H_{\text{max}}$, only the ferromagnetic state is stabilised for the studied materials. The critical transition fields for the hydrides are reduced by more than 50% reference to the pure compounds. This fact indicates that hydrogen stabilizes ferromagnetic couplings. Fig. 3a and b reveal an almost linear temperature dependence of the critical field H_c for AFM to FM state transition.

The magnetic phase transition from helical to the ferromagnetic state in zero field can be explained by the increasing importance of the magnetoelastic forces as well as the basal-plane anisotropy with decreasing temperature [15]. Such a phase transition can be achieved at higher temperatures under the action of a magnetic field.

4. Conclusion

The $\text{Ce}_2\text{Fe}_{17-x}\text{Mn}_x\text{H}_y$ hydrides retain the host alloy symmetry. However, hydrogenation leads to a noticeable lattice expansion and marked modification of the magnetic properties reference to the parent compound. The $\text{Ce}_2\text{Fe}_{17-x}\text{Mn}_x$ compounds undergo an antiferro-ferromagnetic transition either by hydrogenation or by application of external field. The metamagnetic transition fields quench the hydrides in ferromagnetic state in much lower critical fields than observed for the parent compounds. This behaviour indicates that hydrogenation weakens the interlayer antiferromagnetic-like coupling within the dumbbell $6c$ site atoms and thus induces ferromagnetic exchange interactions. The transition temperatures, T_t , T_C of the hydrides strongly increase with hydrogen content as the result of the unit cell volume increase.

Acknowledgements

We are very grateful to S. A. Nikitin and I. S. Tereshina for fruitful discussion.

References

- [1] D. Givord, R. Lemaire, IEEE Trans. Magn. MAG 10 (1974) 109–113.
- [2] O. Isnard, S. Miraglia, C. Giorgetti, E. Dartyge, G. Krill, D. Fruchart, J. Alloys Compd. 262–263 (1997) 198–201.
- [3] Y. Janssen, H. Fujii, T. Ekino, K. Izawa, T. Suzuki, T. Fujita, F.R. de Boer, Phys. Rev. B 56 (21) (1997) 13716–13719.

- [4] T.H. Jacobs, K.H.J. Buschow, G.F. Zhou, J.P. Li, F.R. de Boer, *J. Magn. Magn. Mater.* 104–107 (1992) 1275–1276.
- [5] Y.-g. Wang, F. Yang, C. Chen, N. Tang, P. Lin, H. Xiong, Q. Wang, *J. Magn. Magn. Mater.* 185 (1998) 339–344.
- [6] A.G. Kuchin, A.N. Pirogov, V.I. Khrabrov, A.E. Teplykh, A.S. Ermolenko, E.V. Belozerov, *J. Alloys Compd.* 313 (1–2) (2000) 7–12.
- [7] Z. Arnold, O. Prokhnenko, I. Medvedeva, A. Kuchin, J. Kamarad, *J. Magn. Magn. Mater.* 226–230 (2001) 950–952.
- [8] O. Prokhnenko, Z. Arnold, I. Medvedeva, A. Kuchin, J. Kamarad, *Fizika Nizkikh Temp.* 27 (4) (2001) 375–378.
- [9] O. Isnard, S. Miraglia, J.L. Soubeyroux, D. Fruchart, *J. Less-Common Met.* 162 (1990) 273–284.
- [10] K. Strant, G. Hoffer, A.E. Ray, *IEEE Transactions on Magn.* MAG 2 (3) (1966) 489.
- [11] K. Kulakowski, A. Del Moral, *Phys. Rev. B* 52 (22) (1995) 15943–15950.
- [12] O. Isnard, S. Miraglia, J.L. Soubeyroux, D. Fruchart, P. l’Heritier, *J. Magn. Magn. Mater.* 137 (1994) 151–156.
- [13] H. Fujii, M. Akayama, K. Nakao, K. Tatami, *J. Alloys Compd.* 219 (1995) 10–15.
- [14] O. Isnard, R. Zach, S. Niziol, M. Bacmann, S. Miraglia, J.L. Soubeyroux, D. Fruchart, *J. Magn. Magn. Mater.* 140–144 (1995) 1073–1074.
- [15] H. Fujii, H. Sun, in: K.H.J. Buschow (Ed.), *Handbook of Magnetic Materials*, vol. 9, Elsevier, North-Holland, Amsterdam, 1995.